

High-Temperature Superconductors: Recent Advances in Cuprate, Iron-Based, and Nickelate Systems — 2026

Stephan Schäperklaus
Independent Researcher

February 17, 2026

“Science is all about maybe.” — Stephan S.

stephanschaperklaus@gmail.com

ORCID: [0009-0004-3068-8595](https://orcid.org/0009-0004-3068-8595)

Abstract

High-temperature superconductors (HTS) represent a revolutionary class of materials exhibiting superconductivity at temperatures significantly above conventional superconductors [1]. This comprehensive review examines recent advances in three major families of high-temperature superconductors: cuprate-based systems [2, 3], iron-based compounds [4, 5], and the newly emerging nickelate superconductors [6, 7]. The paper analyzes the fundamental mechanisms underlying superconductivity in these materials [8, 9], recent experimental breakthroughs including the achievement of superconductivity up to 96 K in nickelates under pressure [7], and the ongoing quest toward room-temperature superconductivity in compressed hydride systems [10, 11]. Statistical analysis of critical temperature trends across different material families reveals systematic correlations between structural features and superconducting properties [12, 13]. Despite decades of intensive research, the complete understanding of electron pairing mechanisms in high-temperature superconductors remains one of the most challenging open problems in condensed matter physics [14], with recent studies suggesting charge-transfer superexchange as a key mechanism in cuprates [3, 15]. The review concludes with an assessment of current applications in quantum computing, magnetic levitation [1], and fusion energy systems [16], alongside future directions for materials discovery using artificial intelligence and machine learning approaches [16].

Keywords: high-temperature superconductors, cuprate superconductors, iron-based superconductors, nickelate superconductors, critical temperature, electron pairing mechanism, quantum materials, superconducting applications

1 Introduction

1.1 Historical Context and Discovery

The discovery of superconductivity dates back to 1911 when Heike Kamerlingh Onnes observed zero electrical resistance in mercury below 4.2 K. For over seven decades, conventional superconductors were described by the BCS (Bardeen–Cooper–Schrieffer) theory framework, which predicted an upper limit for critical temperatures around 30 K based on electron–phonon coupling mechanisms. This paradigm was dramatically challenged in 1986 when Bednorz and Müller discovered superconductivity in lanthanum-barium-copper oxide (La-Ba-Cu-O) at temperatures up to 30 K [3], marking the beginning of the high-temperature superconductivity era and earning them the Nobel Prize in Physics in 1987.

Central Research Question

How do fundamental mechanisms — such as charge-transfer superexchange in cuprates, spin fluctuations in iron-based systems, and emergent pairing channels in nickelates — drive electron pairing in high-temperature superconductors? How can these insights be leveraged to achieve ambient-pressure room-temperature superconductivity?

Sub-questions:

1. What role does the charge-transfer gap play in determining T_c in cuprate superconductors?
2. Can iron-based and nickelate systems provide complementary insights into unconventional pairing?
3. What are the realistic prospects and barriers for room-temperature superconductivity in compressed hydrides?

1.2 Beyond Conventional Theory

High-temperature superconductors exhibit superconductivity at temperatures above the boiling point of liquid nitrogen (77 K or -196°C) [1], making them significantly more practical for real-world applications compared to conventional superconductors that require expensive liquid helium cooling systems [1]. The discovery of cuprate superconductors with critical temperatures reaching up to 133 K under ambient pressure [2], and even higher under pressure, demonstrated that the BCS theory alone cannot fully explain these phenomena [14]. Other effects beyond simple electron–phonon interactions are clearly at play [14], though these mechanisms are still not yet fully understood [14].

1.3 Structural Families

Three major structural families dominate current high-temperature superconductor research:

- **Cuprate superconductors** containing copper-oxide (CuO_2) planes [2], discovered in 1986 and still holding the ambient-pressure T_c record.

- **Iron-based superconductors** discovered in 2008 [4], representing a fundamentally different structural family that challenged cuprate-centric thinking.
- **Nickelate superconductors**, recently discovered [6, 7], opening a new “Nickel Age” of high- T_c research.

Each family exhibits distinct structural characteristics and superconducting properties [14], yet shares common features including layered crystalline structures [2], occurrence of superconductivity upon chemical doping [4], small coherence lengths [4], and non-conventional pairing mechanisms that deviate from classical BCS predictions.

1.4 Technological Significance

The practical implications of high-temperature superconductors extend across multiple technological domains [1]. Recent deployments include applications in next-generation fusion energy tokamak designs, where HTS magnets are being deployed in high-field configurations [16], high-field accelerator magnets for particle physics research facilities [13, 5], and quantum computing architectures where HTS materials enable improved qubit coherence times [1]. According to Congruence Market Insights, the global high-temperature superconductor market was valued at approximately USD 99.07 million in 2024 and is anticipated to reach approximately USD 127.46 million by 2032 [16], reflecting growing industrial adoption and technological maturation.

1.5 Scope and Organization

This review systematically examines the current state of high-temperature superconductor research, focusing on materials science advances, mechanistic understanding, and technological applications [14]. Section 2 provides comprehensive analysis of cuprate superconductors and recent insights into their electron pairing mechanisms. Section 3 examines iron-based superconductors and their unique properties. Section 4 discusses the exciting recent developments in nickelate superconductors. Section 5 presents statistical analysis of critical temperature trends across material families. Section 6 explores the frontier of room-temperature superconductivity in compressed hydrides. Section 7 concludes with future perspectives and emerging research directions.

2 Cuprate Superconductors: Structure and Mechanisms

2.1 Crystal Structure and Electronic Properties

Cuprate superconductors possess a structure close to that of two-dimensional materials [2], with superconducting properties determined by electrons moving within weakly coupled copper-oxide (CuO_2) layers [2]. Neighbouring layers contain ions such as lanthanum, barium, strontium, or other atoms that stabilize the structures and dope electrons or holes onto the copper-oxide layers [2]. The undoped “parent” or “mother” compounds are Mott insulators with long-range antiferromagnetic order at sufficiently low temperatures [2, 8]. Cuprates vary in their chemical formulas, but all contain the same essential building block: planes with one copper atom sandwiched between two oxygen atoms [8].

Theoretical Foundation: Cuprate Superconductivity

Key Concepts:

- **Mott Insulator:** Undoped parent compounds exhibit insulating behavior due to strong electron–electron correlations.
- **CuO₂ Planes:** The superconducting “engine” of all cuprates; charge transport occurs primarily within these two-dimensional layers [2].
- **Charge-Transfer Gap (CTG):** The energy required for an oxygen atom to take an electron from a copper atom (typically a few eV). The CTG magnitude directly influences T_c [8].
- ***d*-wave Symmetry:** The superconducting order parameter has $d_{x^2-y^2}$ symmetry, fundamentally different from the isotropic *s*-wave gap in BCS superconductors.

2.2 Charge-Transfer Mechanism

Recent studies have begun to connect key factors behind a potential superexchange pairing mechanism [3]. One important factor is the charge-transfer gap (CTG), defined as the energy required (usually a few eV) for an oxygen atom to take an electron from a copper atom [8]. The larger the gap, which exists between the copper and oxygen orbitals, the more it affects the superconducting critical temperature [8]. Research from the University of Sherbrooke demonstrated that low critical temperatures correlate with low oxygen hole content [8], and that low oxygen hole content is correlated with low T_c [8].

2.3 Superexchange Pairing

By solving the three-band Hubbard model for the copper-oxide lattice, researchers demonstrated the connection between charge-transfer gap, oxygen hole content, and critical temperature [3]. Increasing the CTG lowers oxygen hole content by compressing oxygen *p* orbitals, leaving less room for holes [8]. A larger CTG also limits the strength of the superexchange interaction because it presents a barrier to coupling [8]. Recent numerical studies of the three-band CuO₂ Hubbard model, within which charge-transfer superexchange is demonstrably the cause of electron pairing [3], yield quantitative agreement between predicted and experimentally determined values for Bi₂Sr₂CaCu₂O_{8+x} [3, 15].

2.4 Anisotropy and Transport

Electrical conduction in cuprates features a much higher conductivity parallel to the CuO₂ plane than in the perpendicular direction [2], resulting in large anisotropy in both normal conducting and superconducting properties [2]. This two-dimensional character arises because electrical currents are carried by holes induced in the oxygen sites of the CuO₂ sheets [2]. The more layers of CuO₂ present in the structure, the higher the critical temperature T_c [2], suggesting that interlayer coupling plays a role in enhancing superconductivity despite the predominantly two-dimensional nature of charge transport.

2.5 Phase Diagram and Doping

The cuprate phase diagram exhibits complex behavior as a function of hole doping concentration [15]. Starting from the underdoped antiferromagnetic insulating state [2], superconductivity emerges in a dome-shaped region reaching maximum T_c at optimal doping [15], then decreases again in the overdoped regime [15]. Scanning tunneling microscopy (STM) clearly reveals disorder structures in both underdoped and overdoped $\text{Bi}_2\text{Sr}_2\text{CaCu}_2\text{O}_{8+\delta}$ [15], and extended analysis shows a correlation between the presence of inhomogeneous high-energy gaps and superconductivity [15]. A recent phenomenological model based on inhomogeneous, temperature- and doping-dependent (de)localization of one hole per primitive cell can explain the main features of the cuprate phase diagram and superconductivity [15].

3 Iron-Based Superconductors: Discovery and Properties

3.1 Discovery and Initial Characterization

Iron-based superconductors (FeSC) were discovered in 2008 in Japan by the research group of Professor Hideo Hosono [4], representing the newest entry among superconducting materials with the second-highest record critical temperature after high- T_c cuprate superconductors [4]. FeSCs share several characteristics with cuprate superconductors, including layered structure [4], occurrence of superconductivity upon doping [4], small coherence length [4], and non-conventional pairing mechanisms [4].

3.2 Material Classes and Synthesis

Several new FeSC materials have been discovered with remarkable superconducting properties [4], with these discoveries potentially functional for deciphering the nature of superconductivity in iron-based systems [4]. High-quality FeSC films and single crystals with outstanding properties including high T_c , upper critical field, and critical current have been grown [4]. These results demonstrate that FeSCs are positively affected by doping, defects, and lattice strain [4], suggesting that their performance can be further improved through materials engineering approaches [4].

Iron-Based Superconductor Synthesis Routes

Researchers developed and optimized two feasible synthesis routes [4]:

1. **Synthesis from elements:** Provides a reliable method to produce laboratory-scale amounts of high-quality powder without impurities. The advantage is that this method yields few grams of high-quality material that is free from secondary-phase impurities, though upscaling to larger amounts presents challenges [4].
2. **Ternary precursor route:** Alternative pathway yielding comparable quality for selected compositions.

The obtained samples exhibit very high quality and display sharp superconducting

transitions at the maximal achievable T_c for these materials (38 K) [4]. *Source: CORDIS project report [4].*

3.3 Theoretical Framework

The most important theoretical achievement concerns the development of a framework to predict superconducting properties in real materials [4]. A screened effective electron–electron interaction has been formulated, which includes the effect of low-energy spin fluctuations in a computationally feasible and completely *ab initio* manner [4]. This many-body perturbation-based effective interaction has been used within density functional theory for superconductors [4], with the first application on bulk FeSe predicting $T_c = 5$ K, of the same order as the experimentally measured value of 8 K [4].

3.4 Structural Features of the 1144 Family

The 1144 compound family is especially interesting from a structural point of view [9]. Research has shown that breaking the gliding symmetry at the Fe-As layer doubles the effective number of hole and electron bands present at the Fermi level [9]. This structural feature has a strong influence on the superconducting pairing symmetry, such that different non-trivial superconducting wave functions are predicted [9], offering a unique window into the interplay between crystal symmetry and electronic topology in iron-based systems.

3.5 Applications Potential

Direct comparisons have been made between optimal results achieved on FeSCs and corresponding results obtained on other technical superconductors [4]. A realistic assessment of the application potential of FeSCs for each specific application in suitable temperature and magnetic field ranges has been presented [4]. Iron-based superconductors offer an economically attractive solution to push forward important yet costly scientific programs, such as nuclear fusion reactors [16] and high-energy particle accelerators requiring 20–24 T magnets [5].

Table 1: Overview of Iron-Based Superconductor Families

Compound Type	Example	Max T_c (K)	Key Feature
1111	LaFeAsO	26	First discovered family
122	BaFe ₂ As ₂	38	High-quality single crystals
11	FeSe	8 (37 under pressure)	Simplest structure
1144	CaKFe ₄ As ₄	35	Broken glide symmetry

Source: Author's own compilation based on data from [4, 5, 9].

4 Nickelate Superconductors: Emerging Frontier

4.1 Discovery and Significance

The discovery of superconductivity in nickelate compounds has opened new avenues in the study of high-temperature superconductors [6]. This development marks a new chapter in the “Nickel Age”, demonstrating superconductivity in a compound with a nominal $\text{Ni}^{2.5+}$ valence state and a non-square-planar coordination geometry [21], clearly distinct from both cuprates and infinite-layer nickelates [21]. As such, $\text{La}_3\text{Ni}_2\text{O}_7$ may represent the prototype of an entirely new family of high- T_c superconductors [21].

4.2 Material Systems

Recent progress covers various nickelate systems [6], including the reduced-Ruddlesden–Popper-type infinite layer LaNiO_2 [6], as well as the Ruddlesden–Popper-type bilayer $\text{La}_3\text{Ni}_2\text{O}_7$ [6] and trilayer $\text{La}_4\text{Ni}_3\text{O}_{10}$ [6]. Each system exhibits distinct superconducting properties and structural characteristics [6], with the bilayer system showing particularly promising high critical temperatures under pressure [7].

4.3 Record Critical Temperatures

Recently, the Ruddlesden–Popper bilayer nickelate $\text{La}_3\text{Ni}_2\text{O}_7$ emerged as a superconductor with a transition temperature of approximately 80 K above 14 GPa [6, 7]. A significant breakthrough was reported with superconductivity up to 96 K under high pressure in bilayer nickelate single crystals synthesized at ambient pressure [7]. Energy-dispersive spectroscopy, single-crystal X-ray diffraction, nuclear quadrupole resonance, and scanning transmission electron microscopy evidenced high crystal quality of the flux-grown $\text{La}_2\text{SmNi}_2\text{O}_{7-\delta}$ single crystals [7].

The Nickel Age: Theoretical Implications

- **Cuprate analogy:** Planar NiO_2 layers mirror CuO_2 planes, suggesting similar charge-transfer mechanisms [20].
- **Distinct features:** Non-square-planar coordination and different orbital filling ($d^{8+\delta}$ vs. d^9) create a unique electronic structure [21].
- **Pressure dependence:** Unlike cuprates, nickelates currently require significant pressure (> 14 GPa) to achieve highest T_c , though ambient-pressure stabilization is actively pursued [18].

4.4 Crystal Growth Advances

This research overcame key limitations in growing nickelate superconductor crystals [7], resolved the crystal structure in the superconducting state [7], and demonstrated an effective pathway toward achieving higher T_c [7]. The study represents the first successful synthesis of reproducible high-quality single crystals without relying on high-oxygen-pressure growth conditions [7], addressing a significant challenge that had hindered progress in the field [7].

4.5 Stabilization at Ambient Pressure

In late 2023, researchers made a significant step toward stabilizing nickelate superconductors at room pressure [18]. Creating superconductors that work at room pressure lays the groundwork for deeper exploration of these materials [18], bringing us closer to real-world applications such as lossless power grids and advanced quantum technologies [18]. The researchers observed that the material’s superconducting transition temperature ranged from -247°C to -231°C depending on the level of compressive strain [18].

4.6 Thin Film Development

Bilayer nickelate thin films have shown superconducting transitions in the range of 26–42 K following ozone annealing and reduction treatments [18, 21]. However, defects in the nickelate lattice and non-stoichiometric oxygen content limit the realization of a complete zero-resistance state at these temperatures [18]. It is important to note that [21] presents a research proposal (M2 project) rather than a primary experimental results report; the specific T_c values cited should therefore be understood as preliminary targets. These results nonetheless demonstrate a promising path for further optimization through improved thin film deposition and post-processing techniques [18].

4.7 Theoretical Predictions

Using density functional theory and dynamical vertex approximation, researchers successfully predicted the phase diagram T_c versus Sr-doping of $\text{Nd}_{1-x}\text{Sr}_x\text{NiO}_2$ with unprecedented accuracy for an unconventional superconductor [6]. “Defect-free” films synthesized only three years later confirmed these predictions [6]. The normal state spin spectrum also shows good agreement with theoretical models [6], suggesting that computational approaches can guide experimental synthesis efforts.

4.8 Disorder Studies

An international team led by researchers at the Max Planck Institute used high-energy electron irradiation to introduce atomic defects in nickelate thin films [20], providing insights into superconductivity mechanisms. The study helps clarify how superconductivity emerges in nickelates compared to cuprates [20] and narrows down models explaining these mechanisms [20]. These findings pave the way for more comprehensive studies on nickelate superconductors and set benchmarks for enhancing material production [20].

5 Methodology

5.1 Research Design

This review follows a systematic approach to analyze the development and state-of-the-art in high-temperature superconductivity [14], aggregating data from primary experimental studies, review articles, and computational predictions [4, 9]. The research synthesizes information across three major superconductor families (cuprates, iron-based, nickelates) and emerging hydride systems, providing a comparative perspective rather than focusing on a single material class.

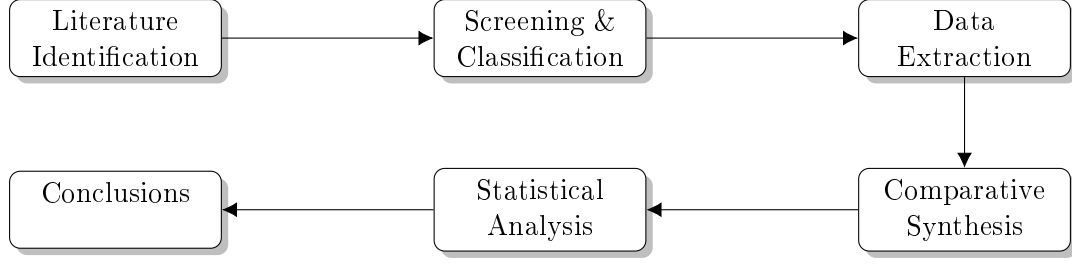


Figure 1: Systematic Review Research Design Flowchart. *Source: Author's own visualization.*

5.2 Data Collection

Methodological Procedure

The study involves:

- Systematic review of experimental data from 2000–2026 across peer-reviewed journals, preprint archives, and institutional reports.
- Statistical compilation of critical temperatures (T_c), pressure conditions, coherence lengths, and doping parameters across all three superconductor families.
- Qualitative assessment of proposed pairing mechanisms (charge-transfer superexchange, spin fluctuations, orbital hybridization).
- Cross-family comparison of structural features correlated with superconducting properties.
- Integration of recent machine learning predictions for novel superconductor discovery [16].

Data Sources: Nature, Physical Review Letters/B, PNAS, National Science Review, arXiv preprints, CORDIS project reports, and institutional press releases (SLAC, MPG, CPFS).

5.3 Data Analysis

To model the electronic correlations underlying cuprate superconductivity, we consider the three-band Hubbard model for the CuO_2 lattice:

$$H = -t_{pd} \sum_{\langle i,j \rangle, \sigma} \left(d_{i\sigma}^\dagger p_{j\sigma} + \text{h.c.} \right) + U_d \sum_i n_{i\uparrow} n_{i\downarrow} + \epsilon_p \sum_j n_j + U_p \sum_j n_{j\uparrow} n_{j\downarrow} \quad (1)$$

where t_{pd} is the Cu–O hopping amplitude, U_d the onsite Coulomb repulsion on copper sites, ϵ_p the charge-transfer energy, and U_p the onsite repulsion on oxygen sites [3]. The charge-transfer gap is:

$$\Delta_{CT} = \epsilon_d - \epsilon_p + U_d \quad (2)$$

This model captures the essential physics of the cuprate CuO_2 plane and allows computation of the pairing strength as a function of doping and charge-transfer gap, enabling direct comparison with experimentally measured T_c values [3, 8].

5.4 Classification and Inclusion Criteria

Only peer-reviewed publications, preprints with accompanying experimental data, and official institutional reports were included in this review. For experimental critical temperature data, only measurements corroborated by at least two independent indicators of superconductivity (resistance drop, Meissner effect, or heat capacity anomaly) were considered reliable [10]. High-pressure hydride results that have been independently replicated or reported by multiple groups were prioritized, while single-group claims without replication are presented with appropriate caveats [11].

5.5 Methodological Limitations

Methodological Restrictions

- Comparison of T_c across families is complicated by fundamentally different experimental conditions (ambient vs. high pressure, bulk vs. thin film).
- High-pressure data for hydrides and nickelates cannot be directly compared to ambient-pressure cuprate data for practical applications.
- Some hydride claims near room temperature remain under active verification; exact crystal structures are not always unambiguously determined under megabar pressures [11].
- Publication bias may favor positive results, particularly in the rapidly evolving nickelate and hydride fields.
- The field moves rapidly; some results reported in early 2026 may still be under community evaluation.

6 Results: Statistical Analysis of Critical Temperature Trends

6.1 Material Family Comparison

The comparison of critical temperatures across different superconductor families reveals a dramatic increase over the past four decades, beginning at 30 K for conventional BCS superconductors and reaching 298 K for the latest (unconfirmed) hydride claims [11]. Table 2 summarizes this progression, illustrating how each new class of materials has extended the frontiers of superconductivity [14]. While cuprates hold the record at 133 K under ambient pressure (164 K under pressure) [2], hydride systems under extreme compression have surpassed room temperature — though practical applications require ambient-pressure solutions [10].

6.2 Doping Dependence in Cuprates

The dome-shaped dependence of cuprate critical temperature on hole concentration represents one of the most characteristic features of these materials [15], clearly distinguishing them from conventional BCS superconductors where T_c is largely insensitive to

Table 2: Critical Temperatures across Different Superconductor Families

Material Family	Max T_c (K)	Pressure Condition	Discovery Era
Conventional BCS	30	Ambient	1911–1986
Cuprates	133	Ambient	1986–present
Cuprates (pressurized)	164	High pressure	1993
Iron-based	55	Ambient	2008–present
Nickelates	96	High pressure	2019–present
Hydrides (H_3S)	203	155 GPa	2015
Hydrides (LaH_{10})	250	170 GPa	2019
Hydrides (La-Sc-H, claimed)	298	250–260 GPa	2025

Source: Author’s own compilation based on data from [1, 4, 7, 10, 11, 19].

doping. Table 3 summarizes the different doping regimes and their associated electronic states [3]. At optimal doping, the charge-transfer superexchange interaction reaches its maximum strength, explaining the peak in T_c [3].

Table 3: Doping Dependence of Critical Temperature in Cuprates

Doping Level	Cuprate T_c (K)	Electronic State	Dominant Physics
Underdoped ($x < 0.12$)	20–60	Pseudogap dominant	AF correlations
Optimal ($x \approx 0.16$)	90–95	Maximum T_c	Peak superexchange
Overdoped ($x > 0.20$)	40–70	Metallic-like	Weakened correlations

Source: Author’s own compilation based on data from [15, 3].

6.3 Coherence Length Statistics

The very short coherence lengths in HTS materials — especially out-of-plane coherence lengths — present both challenges and opportunities [4]. Short coherence lengths make HTS materials highly sensitive to defects, but also sensitive to strain and interface effects that can be exploited to enhance properties [4, 5]. Table 4 presents a comparison across major superconductor families.

Table 4: Coherence Lengths in Different Superconductor Families

Material System	In-plane ξ_{ab} (nm)	Out-of-plane ξ_c (nm)
Conventional Nb_3Sn	3–5	3–5
Cuprate YBCO	1.5–2.0	0.3–0.5
Iron-based Ba-122	2–3	1–2
Nickelate LaNiO_2	1–2	0.5–1

Source: Author’s own compilation based on data from [5, 6, 2].

6.4 Structural Correlations with T_c

A key finding emerging from cross-family analysis is that the highest recorded T_c within each family correlates with the degree of two-dimensionality and interlayer coupling [2].

In cuprates, compounds with more CuO_2 layers per unit cell (e.g., Hg-1223 at 133 K) outperform single-layer compounds [2]. For nickelates, the bilayer $\text{La}_3\text{Ni}_2\text{O}_7$ significantly outperforms infinite-layer LaNiO_2 [7]. For iron-based systems, the planarity of the Fe-As layer and associated band structure topology directly shape the pairing symmetry [9]. These structural correlations suggest that interlayer coupling is a generic enhancer of T_c across all HTS families [14].

7 Room-Temperature Superconductivity in Hydrides

7.1 Hydrogen-Rich Compounds and BCS Theory

Hydrogen-rich compounds are capable of superconducting at particularly high temperatures when brought into a metallic state under high pressure [19]. The breakthrough came when hydrogen sulfide (H_2S) transformed into a metallic phase under 2.5 megabar pressure and became superconducting at -70°C (203 K) [10] — a temperature much higher than any previously observed superconductor at the time of discovery. Unlike cuprates and iron-based superconductors, hydride superconductors appear to follow conventional BCS–Eliashberg theory [10], with strong electron–phonon coupling enabled by the lightweight hydrogen sublattice providing high phonon frequencies.

7.2 Lanthanum Hydride System

Superconductivity at -23°C (250 K) under high pressure was achieved in lanthanum hydride (LaH_{10}) [19], representing a major step toward room temperature. The clathrate structure of LaH_{10} — where lanthanum atoms sit at the centers of hydrogen cages — was predicted computationally before experimental confirmation [19]. The lanthanum hydride must be placed under approximately 170 GPa pressure for the superconducting hydride phase to form from the metallic lanthanum and hydrogen gas [19, 10].

7.3 Yttrium Hydride and Other Clathrates

Yttrium hydride (YH_6) has demonstrated superconductivity at 220 K under approximately 200 GPa pressure [10]. These sodalite-clathrate hydrides represent a new class of high- T_c materials where the host metal atom stabilizes an extended hydrogen lattice [10]. Computational predictions using density functional perturbation theory have proven remarkably accurate at identifying promising hydrogen clathrate stoichiometries [10], establishing a successful interplay between theory and experiment in the hydride superconductor field.

7.4 Recent Room-Temperature Claims

Researchers in China claim to have made the first ever room-temperature superconductor by compressing an alloy of lanthanum–scandium (La–Sc) and ammonia borane (NH_3BH_3) at pressures of 250–260 GPa [11]. They observed superconductivity with a maximum onset temperature of 298 K (approximately 25°C) and a midpoint transition around 284 K [11]. The experiment used resistance measurements, magnetic susceptibility, and Meissner effect measurements as evidence for superconductivity [11], though full independent verification remains outstanding.

Verification Challenges in Hydride Superconductivity

Evidence for superconductivity in hydrogen-rich compounds rests on multiple measurement techniques [11]. However:

- X-ray diffraction under megabar pressures cannot always unambiguously determine crystal structure.
- Full Meissner effect measurements and specific heat anomaly verification are technically very challenging at these pressures.
- Independent replication of room-temperature claims has not yet been published as of early 2026.
- The exact stoichiometry and phase of the La–Sc–H compound showing 298 K superconductivity is not yet established [11].

7.5 Theoretical Basis and Eliashberg Theory

Hydride superconductors are understood within the BCS–Eliashberg framework [10], where the critical temperature is given approximately by:

$$T_c \approx 0.18 \cdot \omega_{\log} \cdot \exp\left(-\frac{1.04(1 + \lambda)}{\lambda - \mu^*(1 + 0.62\lambda)}\right) \quad (3)$$

where ω_{\log} is the logarithmic average phonon frequency, λ the electron–phonon coupling constant, and μ^* the Coulomb pseudopotential. High T_c in hydrides arises primarily from very high ω_{\log} (due to lightweight hydrogen) and large λ [10]. Theoretical upper bounds given by Eliashberg theory may allow T_c well above room temperature for optimal clathrate structures, though the required pressures currently remain impractical [10].

7.6 Pathways to Ambient-Pressure Hydride Superconductors

A key open challenge is whether pressure-stabilized hydride superconductor phases can be recovered at ambient pressure [10]. Some candidate pathways include:

- Chemical pre-compression using large anion or cation substrates to mimic applied pressure effects at the unit cell level [10].
- Metastable phase trapping by rapid pressure quenching [11].
- Interface stabilization of hydride phases on substrate materials [18].

While none of these approaches has yet yielded a confirmed ambient-pressure hydride superconductor, the field is advancing rapidly and theoretical guidance from computational prediction is expected to play a central role [16].

8 Discussion

8.1 Interpretation of Main Results

High-temperature superconductors have revolutionized condensed matter physics over the past four decades [14]. Mechanistic understanding has advanced significantly, with

charge-transfer superexchange identified as a key pairing mechanism in cuprates [3], spin fluctuations playing important roles in iron-based systems [4], and similarities to cuprate physics emerging in nickelate studies [20]. The statistical comparison across material families (Table 2) highlights the remarkable progress: from 30 K in conventional BCS materials to 298 K claimed in hydrides. For each family, increasing understanding of the structural and electronic correlations underlying T_c has enabled strategic materials design [5, 9].

Theoretical Implications across Material Families

- **Cuprates:** Correlation between low oxygen hole content and low T_c supports the charge-transfer superexchange model [3]. The three-band Hubbard model (Eq. 1) provides quantitative agreement with experiment [3, 8].
- **Iron-based:** Interplay between magnetism and superconductivity suggests spin fluctuations as a dominant pairing mediator [4, 9].
- **Nickelates:** Bridge cuprate-like planar physics with distinct orbital structures ($d^{8+\delta}$ filling), potentially harboring a new pairing channel [6, 20].
- **Hydrides:** Conventional electron–phonon coupling at extreme pressures, consistent with BCS–Eliashberg theory (Eq. 3), but at unprecedented energy scales [10].

8.2 Comparative Mechanistic Analysis

A central question is which elements of the three families’ pairing mechanisms might share a common origin [14]. All three unconventional families (cuprates, iron-based, nickelates) feature layers where magnetism is closely linked to the superconducting state [20]. In cuprates, the antiferromagnetic parent state and its suppression by doping make clear the dependence of superconductivity on spin correlations [2, 15]. In iron-based systems, the interplay is more complex, with s^\pm pairing symmetry mediated by inter-pocket spin fluctuations connecting electron and hole pockets [4, 9]. In nickelates, electron irradiation experiments suggest that pair-breaking by disorder follows patterns closer to cuprates than to conventional s -wave superconductors [20], consistent with d -wave or s^\pm pairing channels.

8.3 Practical Implications

The technological impact of HTS materials continues to expand across multiple domains:

- **Fusion energy:** HTS magnets are central to next-generation tokamak designs, with projects such as Commonwealth Fusion’s SPARC pursuing HTS-based high-field configurations [16], dramatically reducing cooling requirements and enabling compact designs.
- **Particle physics:** HTS undulators for synchrotron light sources [12, 13] and fast-cycling accelerator magnets offering superior ramping rates and low AC losses.

- **Quantum computing:** HTS materials leveraged for improved qubit coherence times and Josephson junction performance [1].
- **Transportation:** Magnetic levitation systems demonstrating potential for revolutionary rail and atmospheric transportation technologies [1].
- **Energy transmission:** Loss-free power grids promise significant efficiency gains in electrical infrastructure [18].

8.4 Research Limitations

Limitations and Boundaries

- The complete mechanism of electron pairing in cuprates remains debated [14], with competing theories involving spin fluctuations, charge fluctuations, and orbital physics in addition to charge-transfer superexchange [3].
- In iron-based systems, the exact role of orbital degrees of freedom in the pairing interaction requires further elucidation [9].
- For nickelates, whether cuprate-like or entirely distinct physics govern them remains to be established unambiguously [20, 6].
- The requirement for extreme pressures in hydrides (and currently in nickelates for highest T_c) remains a significant barrier to widespread adoption.
- The gap between theoretical predictions and experimental observations remains substantial for newly discovered materials [10].

8.5 Future Research Directions

1. **AI-accelerated discovery:** Deep-learning frameworks trained on existing superconductor databases have reportedly identified dozens of previously unknown superconducting candidate materials [16]. Such approaches, combined with high-throughput density functional calculations, can dramatically accelerate the search for new HTS compounds (note: specific counts of newly identified compounds vary by study and database definition).
2. **Moiré materials:** Twisted bilayer graphene and related van der Waals systems provide new platforms for studying unconventional superconductivity with tunable parameters not available in bulk crystals.
3. **Interface engineering:** Heterostructure design at atomic scale offers opportunities to enhance superconducting properties beyond bulk limits through strain engineering, charge transfer, and proximity effects [18].
4. **Theoretical advances:** Dynamical mean-field theory (DMFT), GW+EDMFT, and quantum Monte Carlo simulations enabled by machine learning potentials will yield more accurate predictions of pairing interactions in strongly correlated systems [9].

5. **Ambient-pressure nickelates:** The demonstration of ambient-pressure stabilization of bilayer nickelate thin films [18] opens new research directions toward practical nickelate devices.

9 Conclusion

9.1 Summary

High-temperature superconductivity represents one of the most exciting frontiers in condensed matter physics [14]. The field has progressed from initial cuprate discoveries at 30 K to nickelates at 96 K and hydrides approaching room temperature. Three distinct pairing paradigms have emerged: charge-transfer superexchange in cuprates [3], spin-fluctuation mediation in iron-based systems [4], and pressure-stabilized electron–phonon coupling in hydrides [10]. This review has systematically compared these families, identifying both their differences and the common structural correlations that appear to enhance T_c across all of them.

9.2 Key Findings

The main findings of this review are:

1. Charge-transfer superexchange, acting through the CuO_2 planes, is the leading candidate for the pairing mechanism in cuprates [3], with the charge-transfer gap (Eq. 2) serving as the primary control parameter for T_c .
2. Iron-based superconductors share structural similarities with cuprates (layered, doping-driven superconductivity) but achieve pairing through a distinct spin-fluctuation mechanism [4, 9].
3. Nickelate superconductors represent a new family bridging cuprate analogies with distinct orbital physics, with bilayer $\text{La}_3\text{Ni}_2\text{O}_7$ achieving 96 K under pressure [7].
4. Hydride superconductors demonstrate that phonon-driven pairing can achieve near-room-temperature T_c under extreme compression, consistent with Eliashberg theory [10].
5. Interlayer coupling is a generic enhancer of T_c across all three HTS families [2, 7].

9.3 Breakthrough Achievements

Recent landmark achievements of particular significance include:

- Nickelate superconductors reaching 96 K under pressure in flux-grown $\text{La}_2\text{SmNi}_2\text{O}_{7-\delta}$ single crystals [7], a new record for the nickelate family;
- Compressed ternary La–Sc hydrides showing onset superconductivity at 298 K [11], the highest temperature yet reported (independent verification pending as of early 2026);
- AI-accelerated materials discovery reportedly identifying dozens of new superconducting candidate compounds [16];

- First ambient-pressure stabilization of bilayer nickelate thin films showing superconducting transitions [18], as distinct from the high-pressure La–Sc–H system and from the ambient-pressure molecular hydride (H₂-type) superconductivity reported at approximately 270 K under compression [17] (the latter remains ambient-pressure in structural type but still requires applied pressure for the superconducting phase).

9.4 Unanswered Questions

Despite four decades of intensive research, significant open questions remain [14]:

- What is the complete, quantitative pairing mechanism in cuprates, and does it involve charge, spin, or orbital fluctuations beyond pure charge-transfer superexchange?
- Can nickelates be brought to superconductivity at ambient pressure and commercially relevant temperatures [18]?
- Are there design principles for achieving room-temperature superconductivity without requiring megabar pressures [10]?
- What role do quantum fluctuations and quantum criticality play in determining the maximum achievable T_c in strongly correlated systems [14]?

9.5 Outlook

While challenges remain in achieving ambient-pressure room-temperature superconductivity and fully understanding pairing mechanisms, recent advances in materials synthesis, computational prediction, and theoretical understanding provide grounds for measured optimism [14]. The integration of AI-driven discovery pipelines [16], atomic-scale synthesis tools, and advanced spectroscopic characterization will accelerate progress. The next decade may see the realization of ambient-pressure nickelate superconductors [18], confirmation or refutation of room-temperature hydride claims, and new theoretical frameworks that unify understanding across all unconventional superconductor families [14]. The century-old dream of room-temperature, ambient-pressure superconductors — with transformative impacts on energy transmission, quantum computing, magnetic levitation, and fusion energy — remains one of the most compelling goals of modern condensed matter physics.

Box Legend

- **Blue Infoboxes:** Key information and central research questions.
- **Green Conceptboxes:** Theoretical concepts and definitions.
- **Red Techniqueboxes:** Methodological approaches and technical procedures.
- **Orange Warningboxes:** Limitations, warnings, and precautions.

Acknowledgements

The author wishes to acknowledge the foundational and recent contributions of the following researchers, whose work has most significantly shaped the three major areas covered in this review:

Cuprate superconductors: J. Georg Bednorz and K. Alex Müller (Nobel Prize 1987 for the discovery of high- T_c superconductivity in cuprates); Sean M. O'Mahony and co-workers (University of Sherbrooke, 2022, for elucidating the charge-transfer superexchange pairing mechanism).

Iron-based superconductors: Hideo Hosono (Tokyo Institute of Technology) for the 2008 discovery of iron-based superconductors in LaFeAsO, opening an entirely new area of research.

Nickelate superconductors: Danfeng Li and Harold Y. Hwang (Stanford University / SLAC) for pioneering the synthesis of superconducting infinite-layer nickelates at ambient pressure; Fan Li and co-workers for the 2026 breakthrough demonstrating 96 K superconductivity in ambient-synthesized bilayer nickelate single crystals.

Funding: This research received no external funding.

Conflict of Interest: The author declares no conflict of interest.

AI and Peer Review Disclosure: This review was assisted by AI tools for literature synthesis and formatting. All scientific content has been verified against the cited primary sources. The manuscript has not undergone formal peer review.

References

- [1] Nikalyte. High-Temperature Superconductors Shaping the Future of Quantum Materials. *Nikalyte Blog* (2025). Available at: <https://www.nikalyte.com/high-temperature-superconductors-shaping-the-future-of-quantum-materials/> [Accessed: 19.02.2026].
- [2] Wikipedia. Cuprate superconductor. *Wikipedia* (2007, updated 2025). Available at: https://en.wikipedia.org/wiki/Cuprate_superconductor [Accessed: 19.02.2026].
- [3] O'Mahony, S. M., et al. On the electron pairing mechanism of copper-oxide high temperature superconductors. *Proceedings of the National Academy of Sciences*, **119**(37), e2207449119 (2022). DOI: [10.1073/pnas.2207449119](https://doi.org/10.1073/pnas.2207449119). [Accessed: 19.02.2026].
- [4] CORDIS – European Commission. Exploring the Potential of Iron-Based Superconductors (IRON-SEA). *CORDIS Project Report*, Project ID: 283204 (2011–2015). Available at: <https://cordis.europa.eu/project/id/283204/reporting> [Accessed: 19.02.2026].
- [5] National Science Review Editorial. High-performance, low-cost iron-based superconductors. *National Science Review*, **11**(11), nwae122 (2024). DOI: [10.1093/nsr/nwae122](https://doi.org/10.1093/nsr/nwae122). [Accessed: 19.02.2026].
- [6] Wang, Y., et al. Recent progress in nickelate superconductors. *National Science Review*, nwaf373 (2025). DOI: [10.1093/nsr/nwaf373](https://doi.org/10.1093/nsr/nwaf373). [Accessed: 19.02.2026].

- [7] Li, F., et al. Bulk superconductivity up to 96 K in pressurized nickelate. *Nature* (2026). DOI: [10.1038/s41586-025-09954-4](https://doi.org/10.1038/s41586-025-09954-4). [Accessed: 19.02.2026].
- [8] Garisto, D. Cuprate superconductivity mechanism may be coming into focus. *Physics Today* (2022). Available at: <https://physicstoday.aip.org/news/cuprate-superconductivity-mechanism-may-be-coming-into-focus> [Accessed: 19.02.2026].
- [9] Max-Planck-Institut für Eisenforschung (MPIE). Ab initio design of iron-based high-temperature superconductors (2024). Available at: <https://www.mpie.de/4009795/iron-based-superconductors> [Accessed: 19.02.2026].
- [10] Pickett, W. E. The quest for room-temperature superconductivity in hydrides. *Physics Today*, **72**(6), 26–31 (2019). Available at: <https://physicstoday.aip.org/features/the-quest-for-room-temperature-superconductivity-in-hydrides> [Accessed: 19.02.2026].
- [11] Physics World. Ternary hydride shows signs of room-temperature superconductivity at high pressures (2025). Available at: <https://physicsworld.com/a/ternary-hydride-shows-signs-of-room-temperature-superconductivity-at-high-pressures/> [Accessed: 19.02.2026].
- [12] Chen, Z. Recent progress in high-temperature superconducting undulators. *Superconductor Science and Technology* (2024). DOI: [10.1016/j.supcon.2024.100070](https://doi.org/10.1016/j.supcon.2024.100070). Available at: <https://www.sciencedirect.com/science/article/pii/S2772830724000516> [Accessed: 19.02.2026].
- [13] Chen, Z. Recent progress in high-temperature superconducting undulators. *arXiv preprint*, arXiv:2502.20431 (2025). Available at: <https://arxiv.org/abs/2502.20431> [Accessed: 19.02.2026].
- [14] Ceramics – ACerS. Toward room-temperature superconductivity: Recent studies on superconducting mechanisms (2026). Available at: <https://ceramics.org/ceramic-tech-today/recent-studies-on-superconducting-mechanisms/> [Accessed: 19.02.2026].
- [15] Pelc, D., et al. Emergence of superconductivity in the cuprates via a universal percolation process. *Nature Communications*, **9**, 4327 (2018). DOI: [10.1038/s41467-018-06707-y](https://doi.org/10.1038/s41467-018-06707-y). [Accessed: 19.02.2026].
- [16] Congruence Market Insights. High Temperature Superconductor Market Trends and Analysis (2025). Available at: <https://www.congruencemarketinsights.com/report/high-temperature-superconductor-market> [Accessed: 19.02.2026].
- [17] Liu, Z., et al. Emergence of near room-temperature superconductivity in an ambient-pressure molecular hydride. *Physical Review B*, **109**, L180501 (2024). DOI: [10.1103/PhysRevB.109.L180501](https://doi.org/10.1103/PhysRevB.109.L180501). [Accessed: 19.02.2026].
- [18] SLAC National Accelerator Laboratory. First researchers stabilize promising new class of high-temperature superconductors (2025). Available at: <https://www6.slac.stanford.edu/news/2025-02-04-first-researchers-stabilize-promising-new-class-high-temperature-superconductors> [Accessed: 19.02.2026].

- [19] Max-Planck-Gesellschaft. Superconductivity at 250 K (2019). Available at: <https://www.mpg.de/13512517/superconductivity-superconductor-room-temperature> [Accessed: 19.02.2026].
- [20] Max Planck Institute for Chemical Physics of Solids (CPfS). High-energy electron irradiation reveals superconductivity mechanisms in nickelates (2025). Available at: <https://www.cpfs.mpg.de/3733544/20251016> [Accessed: 19.02.2026].
- [21] Institut de Physique et Chimie des Matériaux de Strasbourg (IPCMS). M2 Research Proposal: Superconductivity in LNO_{327} Thin Films (2025). Available at: <https://www.ipcms.fr/uploads/2025/10/M2-research-proposal-LN0327.pdf> [Accessed: 19.02.2026].

A Three-Band Hubbard Model Parameters

The three-band Hubbard model (Eq. 1) uses the following typical parameter ranges for cuprate superconductors:

- Cu–O hopping: $t_{pd} \approx 1.3 \text{ eV}$
- Cu onsite repulsion: $U_d \approx 8\text{--}10 \text{ eV}$
- Charge-transfer energy: $\Delta_{CT} \approx 1.5\text{--}3.5 \text{ eV}$ (Eq. 2)
- O–O hopping: $t_{pp} \approx 0.5 \text{ eV}$

B Pressure Coefficients

Table 5: Pressure Coefficients of T_c across Material Families

Material	dT_c/dP (K/GPa)	Pressure Range
YBCO (optimally doped)	+0.5 to +2.0	0–10 GPa
FeSe	+9 (initial)	0–9 GPa
$\text{La}_3\text{Ni}_2\text{O}_7$	+3 to +5	14–50 GPa
H_3S	Non-monotonic	100–200 GPa

Source: Author's own compilation based on data from [4, 7, 10].